Classical Topological Order in Abelian and Non-Abelian Generalized Height Models

R. Zach Lamberty,[1] Stefanos Papanikolaou,[1,2] and Christopher L. Henley[1]

[1] *LASSP, Cornell University, Ithaca, New York, 14853*

[2] *Dept. of Physics, Yale University, New Haven, Connecticut, 06520*

(Dated: November 1, 2012)

We present Monte Carlo simulations on a new class of lattice models in which the degrees of freedom are elements of an abelian or non-abelian finite symmetry group $\mathcal{G}$, placed on directed edges of a two-dimensional lattice. The plaquette group product is constrained to be the group identity. In contrast to discrete gauge models (but similar to past work on height models) only elements of symmetry-related subsets $\mathcal{S} \in \mathcal{G}$ are allowed on edges. These models have topological sectors labeled by group products along topologically non-trivial loops. Measurement of relative sector probabilities and the distribution of distance between defect pairs are done to characterize the types of order (topological or quasi-LRO) exhibited by these models. We present particular models in which *fully local* non-abelian constraints lead to *global* topological liquid properties.

Introduction: Ever since Wen first proposed that "Topological Order" be considered as a means of classifying chiral spin states in superconductors [1], applications of this "post-Landau" paradigm have caused great excitement in applications to *quantum* systems — the quantum Hall effect [2], fractional quantum Hall effect [3], spin liquids[4–7], and topological quantum computation[8]. Most other physical phenomena, such as critical phenomena, were first understood classically prior to being realized in quantum mechanics, so the question arises whether there is a useful notion of topological order in a *classical* setting. Let us define a generalized topological order in a classical ensemble by the existence of sectors of (energetically or entropically) degenerate states, disconnected in the thermodynamic limit, which cannot be distinguished by any local order parameter. Indeed, one can realize this sort of order in classical models where the inaccessibility is built in by hand, or in a limit where inter-sector transitions are suppressed by an activation energy much larger than the temperature [9, 10]. The motivation for such models is that first, by sharing many features with the quantum models, they provide an arena to do calculations that would not be feasible in the quantum case; secondly, such a classical ensemble can furnish the Hilbert space for contructing a quantum model with the same topological order (e.g. the classical Z_2 topological order in dimer coverings on triangular lattices [11]).

As a particular instance of classical topological ordering, one of us has proposed [10] a new family of models which we will henceforth call "generalized height models" which are based on an abelian or non-abelian *discrete* group in the same way that lattice "height" models [12–16] are based on the integers. These models share many properties of their quantum analogues, including massively degenerate ground states, topological defect charges, and the possibility in non-abelian cases of combining two defect charges in more than one way (called "fusion channels" in the quantum context). In this paper we present simulation results from these models, focused primarily on two measurements which characterize whether a given model is topologically ordered: the relative probabilities of being each sector, and the distribution of separations between a pair of topological defects.

Simulations of the Model: An extended introduction of generalized height models was given previously [10]; here we will outline the properties of a general model and discuss the specific models we have already looked at. Generalized height models can be thought of as lying between height models [12–16] and discrete lattice-gauge models [17]. The former are models in which the vertices of a (not necessarily Bravais) lattice are labeled by finite integer heights (or, conversely, directed edges are labeled by the integer differences between those heights); whereas the latter are defined by elements of general groups assigned to the edges of a lattice (we will later call them "spins").

We can define them via two constraints. These models are generalizations of height models in that the set of integers used in height models to label the degrees of freedom on the edges are replaced by any discrete group (finite or infinite) $\mathcal{G}$ as in gauge models. The "well-defined" constraint of integers around a plaquette adding to zero is thus replaced with the constraint on edge elements $\sigma(\mathbf{r}_i, \mathbf{r}_{i'})$ on edges between vertices at $\mathbf{r}_i$ and $\mathbf{r}_{i'}$ which defines our massively degenerate ensemble:

$$\prod_{i \in Plaq} \sigma(\mathbf{r}_i, \mathbf{r}_{i+1}) = e_{\mathcal{G}}. \tag{C1}$$

This constraint is wholly local, and can be abelian or non-abelian given the group $\mathcal{G}$. If this constraint is violated on a plaquette, that plaquette is said to have a charge defect, with the charge being the plaquette product.

The second constraint is the true novelty of generalized height models. Unlike discrete gauge models, but like height models, *only* elements of a chosen symmetry-related subset

$$\mathcal{S} \subsetneq \mathcal{G} \tag{C2}$$

are placed on the directed edges of the lattice. The set $\mathcal{S}$ is normally a collection of symmetry classes, and is strictly *not* equal to $\mathcal{G}$. Essentially, $\mathcal{S}$ is a symmetry-related subset of elements in $\mathcal{G}$.

In discrete gauge models, all group elements are allowed and therefore spins living on lattice edges may not be correlated with each other (beyond the gauge constraint) as in the toric code [18], for example. The correlations between spins in these restricted spin subset models may be exponentially decaying, but are generally non-trivial. In fact, by changing the size of the allowed spin subset we can discretely interpolate between totally free gauge models and quasi-long range ordered states [19].

Note that constraint C1 implies that elements along any topologically trivial loop in the lattice must multiply to the identity, but it *does not* imply that a topologically non-trivial loop need do so. Our simulations take place on the torus, and we therefore have two independent non-trivial loop products which we take as labels for the disjoint partitions of our ensemble, hereafter referred to as *sectors*. In the case of abelian $\mathcal{G}$, each sector has a uniquely defined label ; for non-abelian groups they are defined up to conjugacy[10]. Local updates (defined precisely below) cannot take us from a configuration in one sector to a configuration in another, but entropically expensive global updates can. Monte Carlo simulations involving updates of these two types provide us with a means of measuring the entropic cost of each sector.

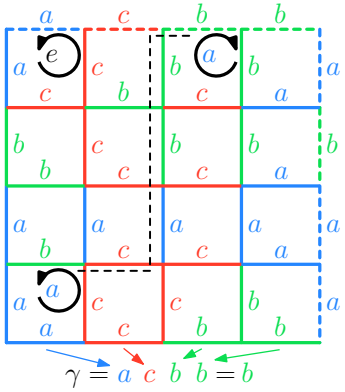

FIG. 1. A sample configuration of our model with group $\mathcal{G} = \mathbb{Z}_2 \times \mathbb{Z}_2$ and spin sub-set $\mathcal{S} = \mathbb{Z}_2 \times \mathbb{Z}_2 \setminus e$ on a periodic square lattice. The upper left plaquette is a "normal" plaquette: the product of the edges is the identity. The lower left and upper middle plaquettes (connected via the black dashed line) are defect plaquettes with opposite "charges" (non-identity plaquette products). We have also shown the plaqutte product along one of the topologically non-trivial loops — this will be half of the "sector" label for this configuration.

In our Monte Carlo simulations, a sequence of local and global update moves (satisfying detailed balance) is used to transition between different configurations. The local move is a single-vertex update in which we multiply all outgoing edges for one vertex by some group value $g \in \mathcal{G}$. This update preserves the plaquette and sector products (up to conjugacy), but is not always allowed (if any of the resulting elements on the outgoing edges are not in the spin set $\mathcal{S}$, that update is rejected).

Transitioning between sectors requires a global move. Our chosen move involves creating a defect / anti-defect pair, randomly walking one around the lattice, and letting them fuse into a new defect (non-abelian models only) or annihilate. The entire process is referred to as a completed defect walk, and an individual jump of a defect from one plaquette to the neighbor as a defect step.

In the case of an Abelian symmetry group $\mathcal{G}$ the defect / anti-defect pair will always annihilate upon coming back together, but in models generated from Non-Abelian symmetry groups they can potentially recombine into a single defect of a different charge. If a defect walks once around some topologically non-trivial loop, every transverse loop gets crossed once and has its loop product changed, so that the new configuration resides in a different sector. Such updates, that change sectors while satisfying detailed balance, allow us to measure the relative weights of the different sectors and thereby ascertain whether the ensemble is topologically ordered.

Constraint C2 induces non-trivial correlations between spins in the lattice, and therefore walking defects may interact with each other through the intermediary spins. Exponentially decaying probability distributions of the distance between defect pairs indicate topologically ordered liquid-like phases with exponentially decaying correlations and deconfined topological defects. Even though we adopt the ensemble of maximum entropy, it is possible that the resulting ensemble has more than topological order [10]: *e.g.* constraints (C1) and (C2) together may so constrain the possibilities in each plaquette that we get a height model, or we could find an emergent long-range ordered phase.

We focus primarily on the square lattice with groups and spin subsets as enumerated in table I. To gauge the difference between models with topological order or with more order, we decided to use the model $\mathcal{G} = \mathbb{Z}_5$ with $\mathcal{S} = \{\pm 1\}$ — which is in a one-to-one mapping with the well-studied six-vertex model (also known as the ice model [20]) — as a benchmark. We ensured that simulations on this model reproduced known values for the six-vertex model before proceeding with possibly topologically ordered models. The other group choices were motivated for different reasons: a model using the three elements of the abelian group $\mathbb{Z}_2 \times \mathbb{Z}_2$ can behave like a three-coloring model in some situations; the group S_3 is the smallest non-abelian group; and $\mathcal{A}_5$ is both the smallest non-abelian simple group (meaning it cannot be "factored" into quotient groups) and is also the symmetry group of the regular icosahedron.

Group $\mathcal{G}$	Spin set $\mathcal{S}$	A or Non-A
$\mathbb{Z}_5$	$\{+1, -1\}$	A
$\mathbb{Z}_2 \times \mathbb{Z}_2$	$\{(0,1),(1,0),(1,1)\}$	A
S_3	All non-identity elements	NA
$\mathcal{A}_5$	All elements of order three	NA

TABLE I. Models simulated for this paper.

In summary, generalized height models offer us two different "tunable" parameters: the local symmetry of the model, as defined by the full group $\mathcal{G}$; and the subset of allowed spins. Each different choice of spin set $\mathcal{S}$ can be thought of as tuning a family of models [19].

Our measurements are based on Monte Carlo simulations of the models with group choices as described in table I and periodic lattices of edge length L. Define a "sweep" of single-site updates as L^2 consecutive single-vertex updates at randomly selected vertices. Global defect walks are performed one step at a time, with the ratio of single-site sweeps to individual steps in the defect random walk specified by hand (for most of the simulations presented in this paper that ratio was 1 sweep per 100 defect steps). We have performed simulations on lattice sizes ranging from 4^2 to 256^2 sites.

Sector Probabilities: By definition, the primary property of topological order in our models is an entropic degeneracy of the lowest energy ensemble in the thermodynamic limit. To demonstrate this, we need some measurement of the relative number of states in different sectors. Completed defect walks traversing a topologically non-trivial path through the system will transition our configuration into a different sector. The relative probability $P(\Gamma)$ that we would find ourselves in sector $\Gamma = (\gamma, \gamma')$ after such a walk then is proportional to the (relative) number of configurations in a sector. A topologically ordered state will have $P(\Gamma)$ converging to a constant value P_∞ independent of Γ as the lattice size L increases; a critical state will have $P(\Gamma)$ converging to different values for different Γ.

In contrast, for models with topological order we expect the probability of being in a sector Γ at any lattice length L to depend on the class, and for those probabilities to decay to each other as a function of lattice size, *i.e.*

$$P(\Gamma, L) = P_\infty(\Gamma) + b^L P_0(\Gamma) \exp\left(-L/\ell(\Gamma)\right), \quad (1)$$

where b^L is a prefactor term which only depends on the even- or odd-ness of L (often $b^L = (-1)^L$). By definition, for a model to be topologically ordered, the number of configurations in each of the N_s sectors must be the same in the thermodynamic limit: $P_\infty(\Gamma) = 1/N_s$ for all Γ.

We start with the benchmark six-vertex model: the number of configurations per sector $\Gamma = (\gamma, \gamma')$[21] in the six-vertex model can be calculated analytically :

$$P(\Gamma, L) \propto \exp\left(-\frac{\kappa}{2}\left(\gamma^2 + \gamma'^2\right)\right), \ \kappa = \frac{\pi}{6}. \quad (2)$$

Note that for any integer height model such as this $P(\Gamma, L)$ is *not* dependent on the lattice edge size L [22]. The constancy as a function of L can be seen in figure 2, and the dependence on the sector Γ in the subset of that figure. Our simulations reproduced a value of $\kappa = .523(1)$.

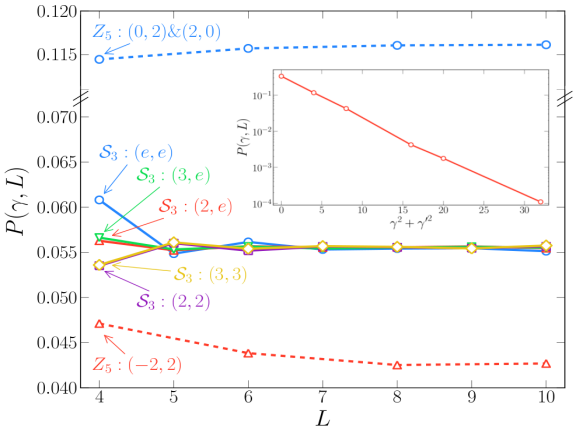

FIG. 2. For the model $S_3(2,3)$ (solid lines), the number of configurations in a sector converges to the same constant value as a function of lattice size L. Though all sectors converge to the same number, at short lattice lengths they behave differently up to the type of group element (*i.e.* the orders of the elements labeled in the figure). For $\mathbb{Z}_5$ (dashed lines), the probability converges to a constant which depends on the sector Γ as $P(\Gamma, L) \propto \exp(-(\kappa/2)(\gamma^2 + \gamma'^2))$. This exponential scaling of sector probabilities for $\mathbb{Z}_5$ is shown in the inset.

The foreground of figure 2 shows the sector probability of the non-abelian $\mathcal{S}_3(2,3)sq$ model. The sector probabilities for different sectors Γ converge to a shared constant value, indicating topological order. The data plotted in figure 2 was averaged over different sectors that are equivalent by symmetry and thus the curves there are labeled not by the group elements of particular sectors but rather by the symmetry class of the element (*e.g.* "2" for order-two elements, "e" for the identity, *etc.*).

Fit values for different sectors for some sectors for a few select models are compiled in table II. *Caution:* simulations of the $\mathcal{A}_5$ model are not fully understood yet, though sector probabilities do appear to be decaying to the same constant value.

Defect Pair Distributions: The constraint (C2) generates non-trivial local correlations. We expect to see exponentially decaying correlations in the topologically ordered models and power law correlations in the $\mathbb{Z}_5$ model.

Γ	$P_0(\Gamma)$	$\ell(\Gamma)$	Γ	$P_0(\Gamma)$	$\ell(\Gamma)$
$\mathcal{G}=\mathbb{Z}_2\times\mathbb{Z}_2, \mathcal{S}=\mathcal{G}\setminus e$			$\mathcal{G}=\mathcal{A}_5, \mathcal{S}=$ Order 2 elem.		
(e,e)	.3138(8)	1.9290(2)	(e,e)	.184(5)	1.63(2)
(a,e)	.0431(1)	2.749(4)	$(e,2)$	.0233(6)	1.96(2)
(a,a)	.01679(9)	4.45(2)	$(e,3)$	.0109(2)	2.44(3)
(a,a')	.1209(4)	1.835(3)	$(e,5_1)$	.0022(8)	3.0(5)
$\mathcal{G}=S_3, \mathcal{S}=\mathcal{G}\setminus e$			$(e,5_2)$	.002(1)	3.1(9)
(e,e)	.45(2)	0.838(7)	$(2,2)$	.048(3)	1.06(2)
$(2,e)$	.061(7)	0.95(3)	$(3,3)$	.0122(5)	1.49(2)
$(3,e)$	.053(3)	0.96(1)	$(5_1,5_1)$	.0131(3)	2.20(3)
$(2,2)$	.097(6)	0.98(1)	$(5_2,5_2)$	.0131(3)	2.20(3)
$(3,3)$	.20(2)	0.86(1)	$(5_1,5_2)$	.0138(2)	2.21(2)

TABLE II. Fit parameters for the assumed exponential fitting form (1) parameters for Abelian and non-Abelian models. The labels Γ are grouped by conjugacy class (not individual element) as sectors are only defined modulo the group conjugacy. The sectors for the S_3 and $\mathcal{A}_5$ simulations are labeled by the order of the conjugacy class ($\mathcal{A}_5$ conjugacy classes 5_1 and 5_2 are related by an outer automorphism), whereas the labels for the $\mathbb{Z}_2\times\mathbb{Z}_2$ model are a for any of the three non-identity elements of that group, and (a,a') when γ and γ' are not the same element.

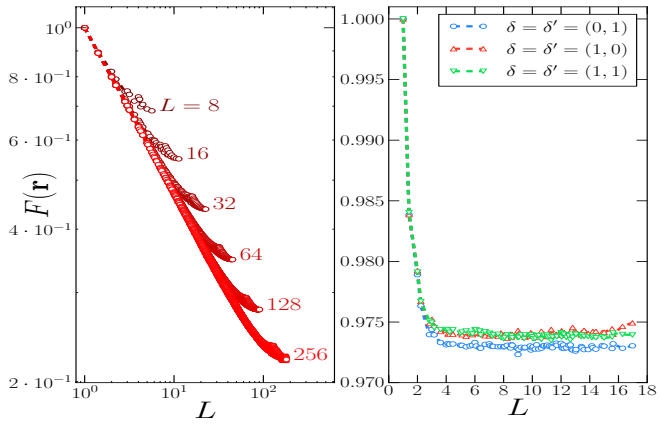

FIG. 3. The left panel shows the defect pair distribution function $F(\mathbf{r})$ for the only defect / anti-defect type possible in the $\mathbb{Z}_5\{\pm1\}sq$ model (+1 and −1) for many different lattice sizes L. The plot is on a log-log scale, clearly indicating the power law behavior. The right panel depicts the defect pair distribution function for the defect types in the $\mathbb{Z}_2\times\mathbb{Z}_2$ model at only $L=24$. The exponential decay is manifested in a rapid decay to a constant background value, indicating deconfinement of defects.

For our topologically ordered models, the defects are deconfined at large distances, but have considerable interactions at short ranges.

The distribution function $F_{\delta,\delta'}(\mathbf{r})$ of the distances between any two defects δ,δ' defines an effective entropic potential $V(\mathbf{r})$ via

$$F_{\delta,\delta'}(\mathbf{r}) = F_0 \exp\left(-V_{\delta,\delta'}(r)\right). \tag{3}$$

For the six-vertex model (here $\mathbb{Z}_5$), we may only have defects of charge ±1, and furthermore it is known that these defects behave like Coulomb charges in two dimensions[12, 23]. The energy required to hold them separate is logarithmic

$$V(\mathbf{r}) \cong -(2/\pi)\kappa \log(\mathbf{r}), \tag{4}$$

with $\kappa=\pi/6$ as noted before , so the pair distribution follows a power law:

$$F_{\pm2,\pm2}(\mathbf{r}) \propto \pm\exp\left(-\frac{1}{3}\log(r)\right) = r^{-1/3}. \tag{5}$$

The power-law behavior can be seen in the distribution functions for the $\mathbb{Z}_5$ model for several lattice sizes L shown in the left panel of figure 3

For topological liquids, on the other hand, exponentially decaying correlations result in a potential which decays exponentially to a constant (that is to say, defects are *deconfined*). This behavior for the $\mathbb{Z}_2\times\mathbb{Z}_2$ model is shown on the right side of figure 3.

Analytical transfer matrix toy calculations [10] suggest that the form of (3) ought to be a sum of exponentially decaying terms. Therefore, we fitted our results to the functional form

$$\log\left(F_{\delta,\delta'}(\mathbf{r})\right) = F^{\infty}_{\delta,\delta'} + F^{0}_{\delta,\delta'}\exp\left(-r/\xi_{\delta,\delta'}\right), \tag{6}$$

with the fit parameters being given in Table III for the models which show the exponentially deconfined defect / anti-defect pair distributions characteristic of TO models.

$\mathcal{G}$	$\mathcal{S}$	δ,δ'	$F^0_{\delta,\delta'}$	$\xi_{\delta,\delta'}$
$\mathbb{Z}_2\times\mathbb{Z}_2$	$\mathbb{Z}_2\times\mathbb{Z}_2\setminus e$	(a,a)	0.170(6)	0.54(2)
S_3	$S_3\setminus e$	$(2,2)$	0.33(9)	0.20(1)
		$(3,3)$	0.11(5)	0.26(4)

TABLE III. TO models feature exponentially decaying defect pair distributions between defect types δ and δ'. Fits were performed on the TO models simulated for this paper and the functional form that was used for the fitting is given in equation (6). For the model $\mathbb{Z}_2\times\mathbb{Z}_2$ we have averaged all three defect / anti-defect pairs; for S_3 we have averaged all pairs of order 2 and order 3 defect / anti-defect pairs, respectively.

Conclusions: Using a generalized definition of topological order, we have explored a new family of classical models which exhibit properties analogous to quantum systems with quantum topological order: (1) topologically robust partitions of massively degenerate ensembles, (2) finite size effects, (3) defect deconfinement (in topological systems), and (4) mediated interactions between charged defects. Elsewhere, we will also exhibit (5)

an ability to "tune" the number of degrees of freedom to transition between topologically ordered and quasi-critical states[19].

Though the applications of topological order are becoming more and more widespread, the number of tractable models that realize topological order is unfortunately still limited. Our generalized height models expand this collection. Furthermore, this non-perturbative approach may be illuminating in unraveling the phenomenology of condensed matter systems where a gauge symmetry is realized only in perturbative limits. Various sorts of quantum models could be constructed from these models (either via the Rokhsar-Kivelson construction[24–26] or the Levin-Wen "string-net" construction [27] Whether the non-abelian models contain anyonic defects depends on the phase factors assigned to the matrix elements in quantizing the generalized height model in question.

Acknowledgements: This work was supported by the National Science Foundation through a Graduate Research Fellowship to R. Zach Lamberty and grant DMR-0552461.

[1] X. G. Wen, Phys. Rev. B, **40**, 7387 (1989).
[2] D. J. Thouless, M. Kohmoto, M. P. Nightingale, M. den Nijs, Phys. Rev. Lett., **49**, 405 (1982).
[3] X.-G. Wen and Q. Niu, Phys. Rev. B, **41**, 9377 (1990).
[4] V. Kalmeyer and R. B. Loughlin, Phys. Rev. Lett., **59**, 2095 (1987).
[5] X.-G. Wen, F. Wilczek, A. Zee, Phys. Rev. B, **39**, 11413 (1989).
[6] N. Read and S. Sachdev, Phys. Rev. Lett., **66**, 1773 (1991).
[7] X.-G. Wen, Phys. Rev. B, **44**, 2664 (1991).
[8] A. Y. Kitaev, Ann. of Phys., **303**, 2 (2003).
[9] C. Castelnovo and C. Chamon, Phys. Rev. B, **76**, 174416 (2007).
[10] C. L. Henley, J. Phys.: Condens. Matter **23**, 164212 (2011).
[11] R. Moessner and S. L. Sondhi, Phys. Rev. Lett. **86**, 1881 (2001).
[12] H. van Beijeren, Phys. Rev. Lett., **38**, 993 (1977).
[13] H. W. J. Blöte and H. J. Hilhorst, J. Phys. A: Math. Gen., **15** L631 (1982).
[14] W. Zheng and S. Sachdev, Phys. Rev. B, **40**, 2704 (1994).
[15] L. Levitov, Phys. Rev. Lett., **64**, 92 (1990).
[16] J. Kondev and C. L. Henley, Phys Rev B., **52**, 6628 (1995).
[17] B. Douçout and L. B. Ioffe, New J. Phys. **7**, 187 (2005).
[18] A. Y. Kitaev, Ann. of Phys., **321**, 2 (2006).
[19] R. Z. Lamberty, S. Papanikolaou, C. L. Henley, unpublished.
[20] Baxter, Rodney J. *Exactly solved models in statistical mechanics.* London: Academic Press Inc. (1982).
[21] In the 6-vertex model (γ, γ') are called "winding numbers" and can be any multiple of 4.
[22] Y. Tang, A. Sandvik, C. L. Henley, Phys. Rev. B, **84**, 174427 (2011).
[23] B. Nienhuis, in *Phase Transitions and Critical Phenomena*, edited by C. Domb and J.L. Lebowitz (Academic, London, 1987), Vol. 11.
[24] D. Rokhsar and S. Kivelson, Phys. Rev. Lett., **61** 2376 (1988).
[25] C. L. Henley, J. Phys.: Condens. Matter **16** S891 (2004).
[26] C. Castelnovo, C. Chamon, C. Mudry, P. Pujol, Ann. of Phys., **318**, 316 (2005).
[27] M. A. Levin and X.-G. Wen, Phys.Rev. B, **71**, 045110 (2005).